

Barrier-controlled thermalization in $\text{In}_{0.53}\text{Ga}_{0.47}\text{As}/\text{InP}$ quantum wells

U. Cebulla, A. Forchel, and G. Bacher

4. Physikalisches Institut, Universität Stuttgart, Pfaffenwaldring 57,
D-7000 Stuttgart 80, Federal Republic of Germany

D. Grützmacher

Institut für Halbleitertechnik, Rheinisch-Westfälische Technische Hochschule Aachen,
D-5100 Aachen 1, Federal Republic of Germany

W. T. Tsang

AT&T Bell Laboratories, 600 Mountain Avenue, Murray Hill, New Jersey 07974-2070

M. Razeghi

Laboratoire Central de Recherches, Domaine de Corbeville, Boîte Postale No. 10,
Thomson-CSF, F91401 Orsay CEDEX, France

(Received 28 March 1989; revised manuscript received 6 June 1989)

We have studied the influence of the barrier thickness on hot-carrier cooling in Nd-YAG (yttrium aluminum garnet) laser-excited $\text{In}_{0.53}\text{Ga}_{0.47}\text{As}/\text{InP}$ quantum wells by picosecond-time-resolved spectroscopy. The experiments yield striking differences of the transient carrier temperatures for different barrier thicknesses. For small barrier thicknesses we observe initial carrier temperatures up to 500 K, whereas for large barrier thicknesses the carrier temperatures stay below 120 K. The experimental data can be explained by microscopic calculations of the transient variation of the carrier densities and the thermalization of hot carriers in the quantum well.

Investigations of hot-carrier cooling in various quantum-well systems are of great interest, as they provide information on optical- and acoustic-phonon scattering, the heating of carriers via Auger processes and the reduction of hot-carrier cooling due to nonequilibrium phonons.¹⁻³ Previous investigations of carrier cooling in $\text{In}_x\text{Ga}_{1-x}\text{As}$ quantum wells^{4,5} have addressed the dependence of hot-carrier cooling on the well width itself. In most of these experiments, no significant influence of the well width on the cooling behavior was observed.

In this paper, we present experimental results for the carrier cooling in $\text{In}_{0.53}\text{Ga}_{0.47}\text{As}/\text{InP}$ quantum wells with different barrier thicknesses. The specific excitation conditions of the $\text{In}_{0.53}\text{Ga}_{0.47}\text{As}/\text{InP}$ samples with a Nd-YAG (yttrium aluminum garnet) laser enables the electrons to diffuse into the InP barrier, whereas the holes are confined to the quantum well.⁶ In Fig. 1 this situation is plotted schematically. Due to the different effective masses of heavy holes and electrons in $\text{In}_x\text{Ga}_{1-x}\text{As}$, about 90% of the laser excess energy is transferred into the electron system. Thus the electrons are created more than about 100 meV above the barrier conduction-band (CB) edge. For wide barriers electrons may diffuse into the InP barrier before they are captured into the quantum well. The electric field between the holes in the $\text{In}_x\text{Ga}_{1-x}\text{As}$ and the moving electrons leads to a drift of the electrons back into the quantum-well layer. Using samples with different barrier thicknesses, we can separate the electron and hole thermalization in the quantum well. The experimental data is in good agreement with calculations for the thermalization, which include the different electron capture in thin and thick barrier samples.

The samples investigated were metal-organic-vapor-phase-epitaxy (MOVPE) and chemical-beam-epitaxy (CBE) (Ref. 7) grown $\text{In}_{0.53}\text{Ga}_{0.47}\text{As}$ quantum wells with well widths L_z between 3.5 nm (Ref. 8) and 8 nm and different InP barrier thicknesses L_B of 20 and 400 nm. Photoluminescence characterizations of these high-quality samples reveal line widths below 5 meV. The samples were excited with a pulse compressed Nd-YAG laser with pulse widths of about 10 ps. For detection of the transient spectra the frequency up-conversion technique was used.

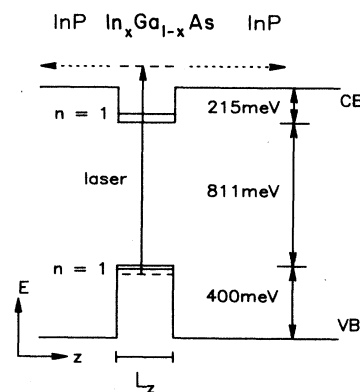


FIG. 1. Schematic band diagram of $\text{In}_{0.53}\text{Ga}_{0.47}\text{As}/\text{InP}$ quantum wells. The broken lines indicate the excitation with a Nd-YAG laser: electrons are created about 100 meV above InP conduction band. The dash-dotted arrows illustrate the diffusion of electrons into the barrier.

All spectra were recorded at a bath temperature of $T_L = 2$ K. An excitation density of about 20 kW cm^{-2} was used in all experiments. Using the absorption constant for $\text{In}_x\text{Ga}_{1-x}\text{As}$ (Ref. 8) we obtain a corresponding hole density on the order of 10^{11} cm^{-2} .

The emissions of quantum wells with similar well widths but different barrier thicknesses reveals distinct differences in the high-energy part of the transient spectra. In Fig. 2 the time-delayed emissions of two samples are compared, consisting of a quantum well with $L_z = 3.5$ nm and barriers $L_B = 20$ nm [Fig. 2(a)] and a sample with a single quantum well of $L_z = 4$ nm with a barrier layer thickness of $L_B = 400$ nm, respectively [Fig. 2(b)].

From the exponential energy dependence of the high-energy part of the luminescence spectra, carrier temperatures T_c for a given time delay have been evaluated. Comparing both sets of spectra one can clearly see that the carrier temperatures T_c differ strongly for similar time delays. For the sample with the large barrier thickness displayed in Fig. 2(b), the initial carrier temperature (10 ps after laser excitation) amounts only to about 110 K. On the other hand, for the sample with the small barriers [Fig. 2(a), $L_B = 20$ nm] the carrier temperature reaches up to $T_c = 460$ K shortly after laser excitation.

In going to longer time delays, the high-energy part of the spectra of samples with different barriers behave quite differently. For large barrier thicknesses the slope of the

high-energy edge of the emission varies slowly with time, whereas for small barrier thicknesses, a rapid decrease of T_c during the first 200 ps is observed.

In Fig. 3, we compare the experimental data for the carrier temperatures versus time delay for different well widths L_z and different barrier thicknesses L_B . For short time delays, we observe carrier temperatures which vary by a factor of about 5 between the samples with thin barriers (see circles in Fig. 3), and thick barriers (triangles in Fig. 3). As demonstrated by the data for quantum wells of 4 and 3.5 nm as well as of 7 and 8 nm well widths, this variation is independent of the well width.

For a quantitative analysis of the cooling curves, we have performed calculations of the carrier temperature within a microscopic model, including the energy loss mechanisms for electrons and holes as well as the transient variation of the carrier densities of electrons and holes. Equation (1) gives the energy-loss mechanisms included in our model

$$\left\langle \frac{dE}{dt} \right\rangle = \frac{1}{\alpha} \left\langle \frac{dE}{dt} \right\rangle_{po} + \left\langle \frac{dE}{dt} \right\rangle_{dp} + \left\langle \frac{dE}{dt} \right\rangle_{pc} + \frac{1}{n} E_g(L_z) n^3 C_A. \quad (1)$$

E_g : transition energy; n : carrier density of electrons or holes; C_A : Auger coefficient; $\langle dE/dt \rangle$: total-energy loss rate for electrons and holes.

The first three terms of Eq. (1) describe the energy loss via LO-phonon scattering (po), deformation potential

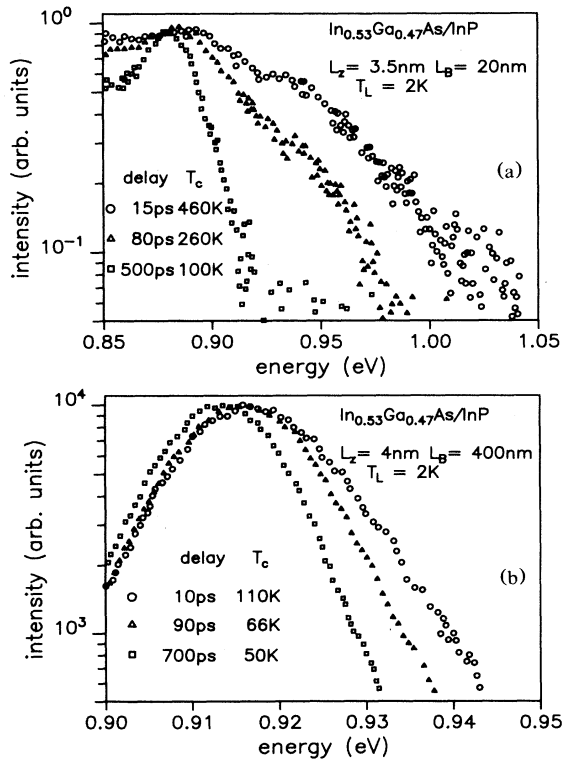


FIG. 2. Luminescence spectra of $\text{In}_{0.53}\text{Ga}_{0.47}\text{As}/\text{InP}$ quantum wells for different time delays after Nd-YAG laser excitation. (a) Sample with $L_z = 3.5$ nm and $L_B = 20$ nm. (b) Sample with $L_z = 4$ nm and $L_B = 400$ nm.

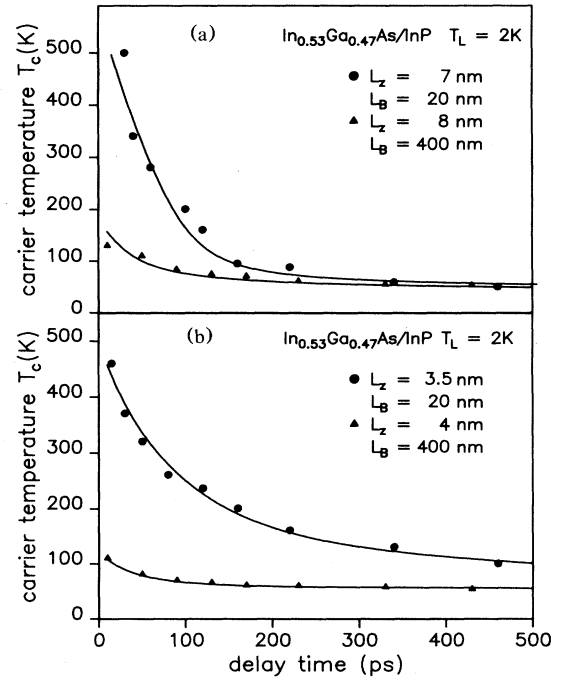


FIG. 3. Carrier cooling curves for two sets of samples with well widths of (a) 7 and 8 nm and (b) 3.5 and 4 nm, with different barrier thicknesses of 20 nm (circles) and 400 nm (triangles). Solid lines: calculations of the carrier cooling curves (see text).

scattering (dp), and piezoelectric scattering (pe), respectively. The last term describes the carrier heating via Auger processes, where an Auger coefficient of $C_A = 5 \times 10^{-29} \text{ cm}^+6\text{s}^{-1}$ has been used.⁹ The factor α is a fitting parameter, taking into account the effective reduction of the carrier cooling due to hot phonon effects. We can only fit our data consistently if we use a value of $\alpha \approx 600$. Similar values have been reported previously for this material system,¹⁰ and corresponds to an effective LO-phonon scattering time of about 70 ps.

In order to include the influence of the different barriers on the transient behavior of the carrier densities, we have developed a simple three level model for the recombination. In this model the influence of the different barrier widths is introduced by a combined capture and relaxation time of the electrons from the InP barrier into the $\text{In}_x\text{Ga}_{1-x}\text{As}$ quantum wells. For the different samples, the capture and relaxation time was determined from fits of the experimentally observed onset of the electron hole plasma emission.⁶ The lifetimes were obtained from the exponential decay of the emission intensity for time delays above about 600 ps.

Figure 4 depicts the calculated electron densities in the $\text{In}_x\text{Ga}_{1-x}\text{As}$ quantum well of $L_z = 4 \text{ nm}$ for different barrier thicknesses using the experimentally determined time constants for the combined capture and relaxation time of the electrons into the quantum well of 50 and 220 ps, corresponding to the two investigated barrier thicknesses of 20 and 400 nm. For the thin barrier (broken line), the electron density reaches a maximum at about 120 ps after laser excitation, whereas for the large barrier of 400 nm (solid line), the maximum of the electron density is significantly delayed. This effect is due to the diffusion of electrons in the InP barrier.

The density of the holes in the $\text{In}_x\text{Ga}_{1-x}\text{As}$ quantum well on the other hand, has its maximum at zero time delay. This is due to the fact that the holes are created resonantly in the $\text{In}_x\text{Ga}_{1-x}\text{As}$ wells. For large time delays, above 600 ps (see Fig. 4), the densities of electrons and holes in the quantum well approach the same value, and finally decay exponentially with the typical recombination lifetime for this quantum well thickness.¹¹

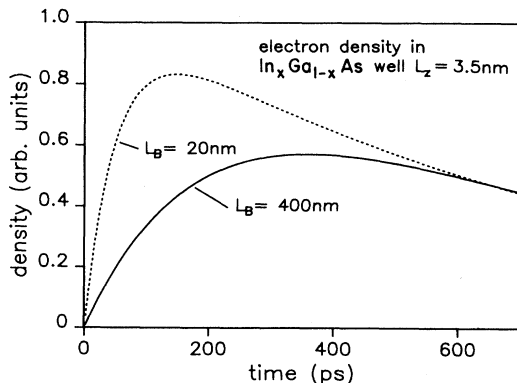


FIG. 4. Transient behavior of the electron density in the $\text{In}_x\text{Ga}_{1-x}\text{As}$ quantum well for different barrier thicknesses: solid line: $L_B = 400 \text{ nm}$; dashed line: $L_B = 20 \text{ nm}$.

It is necessary to introduce the transient behavior of the electron and hole densities in our calculations for the corresponding sample, to achieve a consistent fit to the experimental data. From Eq. (1), we calculate the carrier temperatures for electrons $T_e(t)$ and holes $T_h(t)$. For a certain time delay Δt the carrier temperature $T_c(t + \Delta t)$ can be obtained by using Eq. (2),¹² assuming an instantaneous thermalization of electrons and holes to a common T_c

$$T_c(t + \Delta t) = \frac{n(t)E_e(t) + p(t)E_h(t)}{n(t)E_e(t)/T_e + p(t)E_h(t)/T_h}, \quad (2)$$

where $E_{e,h}(t)$ describes the mean energy of electrons and holes. In Eq. (2), we take into account that the densities of electrons $n(t)$ and holes $p(t)$ in the quantum well may not be equal at a certain time delay, as electrons may diffuse in the barrier.

The solid lines in Fig. 3 have been calculated from Eqs. (1) and (2), using the same standard energy loss rates for the different scattering mechanisms and including the different temporal variation of the electron densities in samples with thick and thin barriers as displayed in Fig. 4. The good agreement of experimental and theoretical data for both barrier geometries demonstrates that the observed drastic differences in the thermalization are due to the influence of the barrier on the carrier cooling.

Physically, the influence of the transient variation of the densities of electrons and holes on the cooling of hot carriers results from the different excess energies in conjunction with the different energy loss rates for electrons and holes. For large barrier thicknesses the electrons move significantly into the InP barrier whereas the holes are kept confined to the quantum well. Therefore, the cooling of holes occurs immediately after the laser pulse. Moreover, the energy loss rates for holes are considerably larger than those for electrons.¹³ On the other hand, cooling of the electrons occurs only after the capture into the quantum well. This leads to a separation of the thermalization time scales of electrons and holes for large barriers. The gradual increase of the electron concentration corresponds to a small energy flux into the cold hole system and hence only low plasma temperatures are obtained.

For small barrier thicknesses, electron and hole densities are equal shortly after the laser pulse, and no significant diffusion into the barrier occurs. In this case synchronous thermalization of electrons and holes takes place, resulting in high initial carrier temperatures of $T_c \approx 500 \text{ K}$.

In summary we have demonstrated experimentally and by model calculations, that the cooling of hot carriers in $\text{In}_{0.53}\text{Ga}_{0.47}\text{As}/\text{InP}$ quantum wells is strongly influenced by the barrier geometry of the samples. By using a Nd-YAG laser, electrons and holes can be spatially separated due to the possibility of a diffusion of the electrons into the InP barrier. The delayed capture of electrons into the $\text{In}_x\text{Ga}_{1-x}\text{As}$ quantum well for large barrier thicknesses leads to the formation of a cold electron hole plasma with initial carrier temperatures below 110 K. For small barrier thicknesses on the other hand, the synchronous thermalization of electrons and holes gives rise to an electron hole plasma with high initial carrier temperatures ($T \approx 500 \text{ K}$).

We would like to thank M. Pilkuhn and P. Balk for stimulating discussions. The financial support of this work by Standard Electric Lorentz AG (SEL) is gratefully appreciated.

-
- ¹W. Pötz and P. Kocevar, *Phys. Rev. B* **28**, 7040 (1983).
²J. Shah, *IEEE J. Quantum Electron.* **QE-22**, 1728 (1986).
³P. J. Price, *Superlattices Microstruct.* **3**, 255 (1985).
⁴H. Lobentanzer, H. J. Polland, W. W. Rühle, W. Stolz, and K. Ploog, *Appl. Phys. Lett.* **51**, 673 (1987).
⁵D. J. Westland, J. F. Ryan, M. D. Scott, J. I. Davies, and J. R. Riffat, *Solid State Electron.* **31**, 431 (1988).
⁶U. Cebulla, G. Bacher, A. Forchel, H. Jürgens, and M. Razeghi, *Appl. Phys. Lett.* **55**, 933 (1989).
⁷W. T. Tsang and E. F. Schubert, *Appl. Phys. Lett.* **49**, 220 (1986).
⁸M. Razeghi, J. P. Hirtz, U. O. Ziemels, C. Delalande, B. Etienne, and M. Voos, *Appl. Phys. Lett.* **43**, 585 (1983).
⁹E. Zielinski, F. Keppler, S. Hausser, M. Pilkuhn, R. Sauer, and W. T. Tsang, *IEEE J. Quantum Electron.* **QE-25**, 1407 (1989).
¹⁰H. Lobentanzer, W. W. Rühle, H. J. Polland, W. Stolz, and K. Ploog, *Phys. Rev. B* **36**, 2954 (1987).
¹¹U. Cebulla, G. Bacher, A. Forchel, and W. T. Tsang, *Phys. Rev. B* **39**, 6257 (1989).
¹²K. Leo and W. W. Rühle, *Solid State Commun.* **62**, 659 (1987).
¹³J. Shah, A. Pinczuk, A. C. Gossard, and W. Wiegmann, *Phys. Rev. Lett.* **54**, 2045 (1985).